

Carbon–Carbon Bonds Functioning as Electron Shuttles: The Generation of Electron-Rich Manganese(II)–Schiff Base Complexes and Their Redox Chemistry

Emma Gallo,[†] Euro Solari,[†] Nazzareno Re,[‡] Carlo Floriani,^{*,†}
 Angiola Chiesi-Villa,[§] and Corrado Rizzoli[§]

Contribution from the Institut de Chimie Minérale et Analytique, BCH, Université de Lausanne, CH-1015 Lausanne, Switzerland, Dipartimento di Chimica, Università di Perugia, I-06100 Perugia, Italy, and Dipartimento di Chimica, Università di Parma, I-43100 Parma, Italy

Received November 27, 1996[⊗]

Abstract: The reduction of [Mn(II)-salophen] derivatives [salophen = *N,N'*-ethylenebis(salicylideneaminato) dianion] led to the formation of C–C bridged dimers. Such C–C bonds function as two electron shuttles in electron-transfer reactions. The reduction of [Mn(salophen)(THF)]₂ (**1**) and [Mn(3,5-Bu^t₄salophen)(THF)]₂ (**3**) with 2 equiv of sodium metal led to the corresponding single C–C bond bridged dimers, [Mn₂(salophen)₂Na₂(DME)₄] (**5**) [salophen₂ = C–C bonded salophen dimer] and [Mn₂(3,5-Bu^t₄salophen)₂Na₂(DME)₆] (**7**), respectively. Complexes **5** and **7** undergo a further two electron reduction to [Mn₂(*salophen*)Na₄(DME)₆] (**6**) [*salophen* = C–C doubly bonded salophen dimer] and [Mn₂(*3,5-Bu^t₄salophen*)Na₄(DME)₄] (**8**), respectively, both containing a double C–C bridge. The obtention of [Mn₂{salophen(Me)CH₂}]₂Na₄(DME)₄] (**9**) from [Mn(salophen-Me₂)(THF)]₂ (**2**) strongly supports the existence of free radical precursors in the formation of C–C bonds. Complex **6** has been used as a source of four electrons in a number of reactions, thus reduction of Ag⁺, PhCH₂Cl, *p*-benzoquinone, and [Co^{II}(MeOsalen)] occurs with the regeneration of the starting material **1**. The C–C bond cleavage is the source of electrons, without being involved in any reaction as a reactive site. With stronger oxidizing agents not only complexes **6** and **8** transfer the electrons stored at the C–C bonds but also the metal undergoes a change in the oxidation state. The reaction of **6** with dioxygen produces a novel form of di-*μ*-oxo-Mn(IV) dimers, where the salophen ligand displays a bridging bonding mode in [Mn₂(*μ*-salophen)₂(*μ*-O)₂] (**15**) and [Mn₂(*μ*-3,5-Bu^t₄salophen)₂(*μ*-O)₂] (**16**).

Introduction

The chemistry presented in this paper concerns the design of molecules which contain at the same time an active site like a transition metal and an additional functionality which is devoted to the storage and delivery of electrons. The latter one should be different from the metal itself. To couple a metal and an independent electron reservoir in the same molecule may open attractive perspectives in the molecular design of molecules devoted to energy storage (molecular batteries) or for a functioning mode in charge storage different from that in Photosystem II.¹

Let us consider the most common mechanisms by which we can store and release electrons from molecules. The most obvious involves changing the oxidation state of the metal, thus a number of single electrons are made available at different potentials. Another, though from an organic perspective, involves the use of polyaromatic systems able to accept electrons in the π^* orbitals, though this is limited in its storage capacity.² A third possibility concerns the formation and cleavage of chemical bonds. This latter mechanism would make available electron in pairs and relatively large in number. The reductive

or the oxidative coupling and their reverse, which are well-known classes of reaction in organometallic chemistry, can be used for the formation and cleavage of bonds. A significant example comes from the natural redox relationship between cysteine and cystine.³

We report here how we can store electrons in the formation of the most common C–C bonds, *via* the reversible reductive coupling of imino groups belonging to a tetradentate Schiff base ligand, that is salophen [*N,N'*-ethylenebis(salicylideneaminato) dianion] bonded to manganese(II). This observation has been made, though not exhaustively explored, by us in the past in some reductions of Ni–, V–, and Co–salophen complexes.⁴ These C–C bonds are oxidatively cleaved in a number of reactions, without being directly involved as reactive sites in the same reaction. To couple Mn and an intramolecular electron reservoir may be of relevant significance in designing artificial Photosystems II.¹

We give here an account on the electron-rich manganese(II) derived from the stepwise reduction of the model compounds: [Mn(salophen)(thf)₂] and [Mn(3,5-Bu^t₄salophen)(thf)₂] and their behavior on the reoxidation using mainly dioxygen and quinones. A few of the present results have been briefly communicated.⁵

* To whom correspondence should be addressed.

[†] University of Lausanne.

[‡] University of Perugia.

[§] University of Parma.

[⊗] Abstract published in *Advance ACS Abstracts*, May 1, 1997.

(1) (a) *Photosynthesis*; Briggs, W. R., Ed.; ARL: New York, 1989. (b) *The Photosynthetic Reaction Center*. Deisenhofer, J., Norris, J. R., Eds.; Academic: New York, 1993 Vol. I and II. (c) *Manganese Redox Enzymes*; Pecoraro, V. L., Ed.; VCH: New York, 1992. (d) Wieghardt, K. *Angew. Chem., Int. Ed. Engl.* **1989**, 28, 1153.

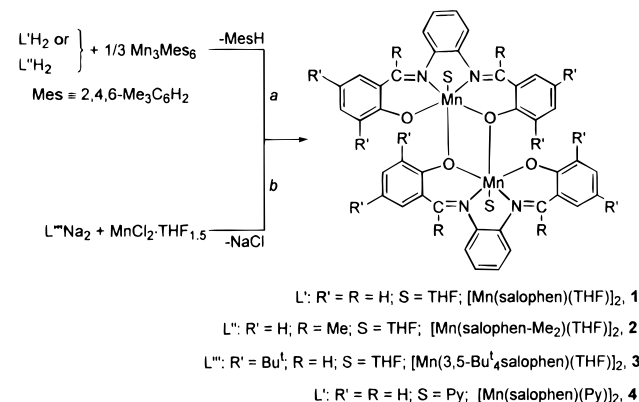
(2) (a) Foster, R. *Organic Charge Transfer Complexes*; Academic: London, 1969. (b) Miller, L. L.; Mann, K. R. *Acc. Chem. Res.* **1996**, 29, 417.

(3) Fluharty, A. L. In *The chemistry of the thiol group*; Patai, Ed.; Wiley: London, 1974; Chapter 13, p 601.

(4) Gambarotta, S.; Floriani, C.; Chiesi-Villa, A.; Guastini, C. *J. Chem. Soc., Chem. Commun.* **1982**, 756. (b) Gambarotta, S.; Urso, F.; Floriani, C.; Chiesi-Villa, A.; Guastini, C. *Inorg. Chem.* **1983**, 22, 3966. (c) Gambarotta, S.; Mazzanti, M.; Floriani, C.; Zehnder, M. *J. Chem. Soc., Chem. Commun.* **1984**, 1116. (d) De Angelis, S.; Solari, E.; Gallo, E.; Floriani, C.; Chiesi-Villa, A.; Rizzoli, C. *Inorg. Chem.* **1996**, 35, 5995 and references therein.

(5) Gallo, E.; Solari, E.; De Angelis, S.; Floriani, C.; Re, N.; Chiesi-Villa, A.; Rizzoli, C. *J. Am. Chem. Soc.* **1993**, 115, 9850.

Scheme 1



Results and Discussion

1. Starting Compounds. The synthesis of compounds **1** and **2** has been carried out using an organometallic method (in Scheme 1, *a*) in order to avoid (i) the presence of alkali and ammonium salts in the final product; (ii) protic conditions; and (iii) separation of poorly soluble final products from salts. This method is now particularly convenient, due to the scaled up synthesis of Mn_3-Mes_6 , [$Mes \equiv 2,4,6-Me_3C_6H_2$].⁷

In the case of **3**, its high solubility allowed the use of the conventional metathetical reaction with $MnCl_2$ for the synthesis (Scheme 1, *b*). Complexes **1–3** have been isolated as dimers in their solvated form with THF, which can be easily replaced by other solvents like pyridine in **4**. The structure of such dimeric forms is exemplified by the report on the X-ray analysis of **4**, while the magnetic properties will be discussed along with those of the other dimers reported through the paper. Selected bond distances and angles are quoted in Tables 1–4 for complexes **4–6**, and **9**, respectively. In Table 5 a comparison of relevant conformational parameters is given for all complexes. We anticipate that complex **4** consists of discrete dimeric units (Figure 1). Manganese exhibits a pseudo-octahedral coordination with the N_2O_2 set of atoms from the salophen ligand in the equatorial plane and the pyridine molecule in an axial position, while the sixth coordination site is occupied by the oxygen of a second monomeric unit at a rather long distance [Mn1A–O1B, 2.262(12) Å; Mn1B–O1A, 2.254(13) Å]. For the structural Mn–O, and Mn–N parameters we refer to Table 1, since they are in the range expected for Mn(II)–Schiff base complexes.^{8,9} The N_2O_2 core is not planar, showing remarkable tetrahedral

Table 1. Selected Bond Distances (Å) and Angles (deg) for Complex **4**

	molecule A	molecule B	
Mn1–O1	2.087(10)	2.097(10)	
Mn1–O2	2.062(13)	2.015(13)	
Mn1–N1	2.217(17)	2.238(16)	
Mn1–N2	2.212(18)	2.200(17)	
Mn1–N3	2.382(15)	2.387(15)	
O1–C1	1.31(2)	1.36(2)	
O2–C20	1.30(3)	1.31(3)	
N1–C7	1.31(3)	1.27(3)	
N1–C8	1.41(3)	1.41(3)	
N2–C13	1.46(3)	1.43(3)	
N2–C14	1.26(3)	1.33(3)	
N3–C21	1.31(3)	1.36(3)	
N3–C25	1.36(3)	1.34(3)	
N1–Mn1–N2	73.2(7)	75.1(6)	
O2–Mn1–N2	86.3(6)	85.4(6)	
O2–Mn1–N1	159.2(6)	160.0(6)	
O1–Mn1–N2	158.2(7)	159.0(6)	
O1–Mn1–N1	85.9(5)	84.9(5)	
O1–Mn1–O2	114.8(5)	115.0(5)	
Mn1–O1–C1	124.4(11)	125.6(11)	
Mn1–O2–C20	130.8(13)	132.2(13)	
Mn1A–O1B	2.262(12)	Mn1B–O1A	2.254(13)
N3A–Mn1A–O1B	169.3(6)	N3B–Mn1B–O1A	169.3(5)
Mn1A–O1A–Mn1B	102.2(4)	Mn1A–O1B–Mn1B	101.6(4)
C1A–O1A–Mn1B	114.5(11)	C1B–O1B–Mn1A	115.2(11)

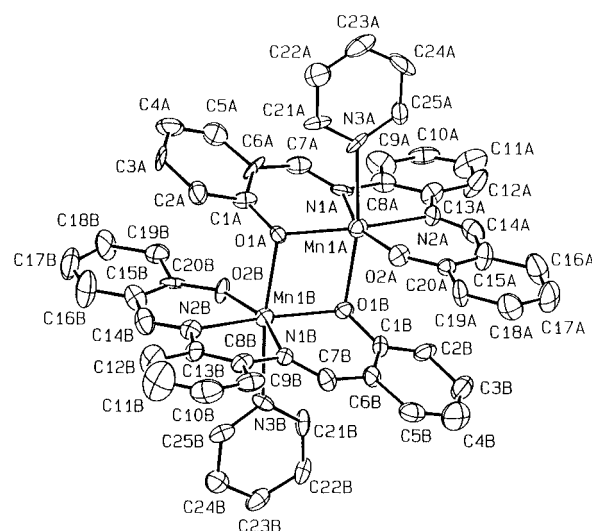


Figure 1. ORTEP view of complex **4**.

distortions (Table 5). Each [Mn(salophen)] moiety assumes a twisted “umbrella” conformation, the dihedral angles between peripheral phenolic rings being 19.0(7) and 21.8(8)° for moiety A and B, respectively.

The temperature dependence of the magnetic moments of the starting compounds **1–4** are typical of weakly coupled Mn(II) dimers. The data of **3**, taken as representative of the four compounds (**1–4**), were fitted with the simple theoretical equation¹⁰ obtained by the Heisenberg spin hamiltonian $H_{ex} = -2J\hat{S}_1 - \hat{S}_2$, with $S_1 = S_2 = 5/2$. To obtain a good fitting, we included a correction for a small quantity of monomeric Mn(II) impurities, x , which were assumed to obey Curie law, obtaining $g = 1.97$, $J = -4.7 \text{ cm}^{-1}$, and $x = 1.8 \%$.¹¹

2. Reduced Forms of [Mn(salophen)] Derivatives. Complex **1** undergoes a stepwise reduction to **5** and **6** in the reaction with sodium metal in THF. The sequence is pictorially shown

(10) O'Connor, C. J. *Progr. Inorg. Chem.* **1982**, *29*, 203.

(11) A detailed report on the magnetic properties of all the dimeric compounds cited in this paper is in the Supporting Information.

(6) (a) Guerriero, P.; Tamburini, S.; Vigato, P. A. *Coord. Chem. Rev.* **1995**, *139*, 17. (b) Floriani, C.; Calderazzo, F.; Randaccio, L. *J. Chem. Soc., Chem. Commun.* **1973**, 384. (c) Gambarotta, S.; Corazza, F.; Floriani, C.; Zehnder, M. *J. Chem. Soc., Chem. Commun.* **1984**, 1305. (d) Horwitz, C. P.; Ciringh, Y. *Inorg. Chim. Acta* **1994**, *225*, 191. (e) Bresciani-Pahor, N.; Calligaris, M.; Delise, P.; Nardin, G.; Randaccio, L.; Zotti, E.; Fachinetti, G.; Floriani, C. *J. Chem. Soc., Dalton Trans.* **1976**, 2310. (f) Horwitz, C. P.; Warden, J. T.; Weintraub, S. T. *Inorg. Chim. Acta* **1996**, *246*, 311–320. (g) Giacomelli, A.; Floriani, C.; Perego, G. *J. Chem. Soc., Chem. Commun.* **1982**, 650. (h) Solari, E.; Floriani, C.; Cunningham, D.; Higgins, T.; McArdle, P. *J. Chem. Soc., Dalton Trans.* **1991**, 3139. (i) Gibney, B. R.; Wang, H.; Kampf, J. W.; Pecoraro, V. L. *Inorg. Chem.* **1996**, *35*, 6184.

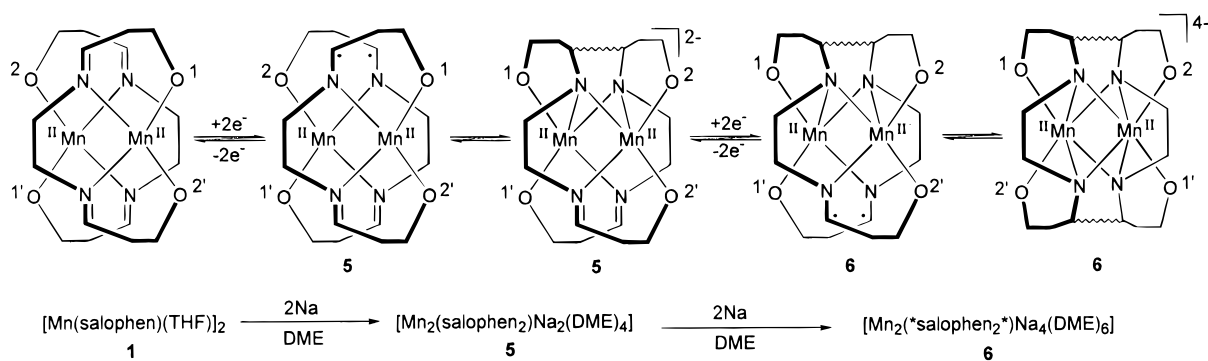
(7) Solari, E.; Musso, F.; Gallo, E.; Floriani, C.; Re, N.; Chiesi-Villa, A.; Rizzoli, C. *Organometallics* **1995**, *14*, 2265.

(8) Srinavan, K.; Michaud, J. K. *J. Am. Chem. Soc.* **1986**, *108*, 2309.

(9) (a) Luaces, L.; Bermejo, M. R.; Garcia-Vazquez, J. A.; Romero, S.; Sousa, A.; Watkinson, M.; Mugnier, Y.; McAuliffe, C. A.; Pritchard, R. G.; Helliwell, M. *Polyhedron* **1996**, *15*, 1375. (b) Higuchi, C.; Sakiyama, H.; Okawa, H.; Isobe, R.; Fenton, D. E. *J. Chem. Soc., Dalton Trans.* **1994**, 1097. (c) Kessissoglou, D. P.; Butler, W. M.; Pecoraro, V. L. *Inorg. Chem.* **1987**, *26*, 495. (d) Mabad, B.; Cassoux, P.; Tuchagues, J.-P.; Hendrickson, D. N. *Inorg. Chem.* **1986**, *25*, 1420. (e) Gallo, E.; Solari, E.; Floriani, C.; Chiesi-Villa, A.; Rizzoli, C. *Organometallics* **1995**, *14*, 2156.

Table 2. Selected Bond Distances (Å) and Angles (deg) for Complex **5**

Mn1–O1	2.036(7)	Mn2–O2	1.995(7)		
Mn1–O4	2.027(6)	Mn2–O3	2.011(7)		
Mn1–N1	2.208(10)	Mn2–N3	2.213(8)		
Mn1–N2	2.135(7)	Mn2–N2	2.182(6)		
Mn1–N4	2.184(9)	Mn2–N4	2.143(8)		
Na1–O1	2.353(6)	Na2–O2	2.401(8)		
Na1–O4	2.525(6)	Na2–O3	2.398(7)		
Na1–O5	2.458(9)	Na2–O7	2.403(11)		
Na1–O6	2.304(14)	Na2–O8	2.438(11)		
		Na2–O9	2.611(13)		
		Na2–O10	2.405(12)		
O1–C1	1.336(13)	O3–C21	1.329(12)		
O2–C20	1.351(12)	O4–C40	1.355(13)		
N1–C7	1.281(14)	N3–C27	1.306(13)		
N1–C8	1.437(12)	N3–C28	1.394(14)		
N2–C13	1.378(14)	N4–C33	1.367(14)		
N2–C14	1.443(14)	N4–C34	1.508(11)		
C14–C34	1.602(15)				
C14–C15	1.543(13)	C34–C35	1.504(11)		
N2–Mn1–N4	69.8(3)	N2–Mn2–N4	69.6(3)	O3–Na2–O10	96.9(3)
N1–Mn1–N4	131.5(3)	N2–Mn2–N3	129.5(3)	O3–Na2–O9	97.8(3)
N1–Mn1–N2	74.8(3)	N3–Mn2–N4	73.0(3)	O3–Na2–O8	163.4(4)
O4–Mn1–N4	94.8(3)	O2–Mn2–N2	93.0(3)	O3–Na2–O7	97.0(3)
O4–Mn1–N2	106.6(3)	O2–Mn2–N4	109.0(3)	O2–Na2–O10	100.0(3)
O4–Mn1–N1	126.9(3)	O2–Mn2–N3	131.1(3)	O2–Na2–O9	164.6(4)
O1–Mn1–N4	118.8(3)	O3–Mn2–N2	120.3(3)	O2–Na2–O8	104.4(3)
O1–Mn1–N2	156.2(3)	O3–Mn2–N4	155.4(3)	O2–Na2–O7	105.0(4)
O1–Mn1–N1	84.5(3)	O3–Mn2–N3	84.8(3)	O2–Na2–O3	74.8(3)
O1–Mn1–O4	95.1(2)	O2–Mn2–O3	93.4(3)		
O5–Na1–O6	69.1(4)	O9–Na2–O10	67.0(4)		
O4–Na1–O6	100.3(3)	O8–Na2–O10	99.5(4)		
O4–Na1–O5	169.1(3)	O8–Na2–O9	86.5(4)		
O1–Na1–O6	107.2(4)	O7–Na2–O10	153.8(4)		
O1–Na1–O5	104.6(3)	O7–Na2–O9	89.1(4)		
O1–Na1–O4	75.8(2)	O7–Na2–O8	67.0(4)		
Mn1–N2–Mn2	81.0(3)	Mn1–N4–Mn2	80.8(3)	N2–C14–C34	108.2(7)
Mn2–N2–C14	101.4(6)	Mn2–N4–C34	112.7(5)	N2–C14–C15	117.0(8)
Mn2–N2–C13	119.4(6)	Mn2–N4–C33	115.6(5)	C15–C14–C34	113.0(8)
Mn1–N2–C14	113.0(5)	Mn1–N4–C34	102.3(6)	N4–C34–C14	103.2(7)
Mn1–N2–C13	113.6(6)	Mn1–N4–C33	121.4(5)	N4–C34–C35	117.3(7)
C13–N2–C14	121.1(8)	C33–N4–C34	118.0(8)	C14–C34–C35	113.5(8)

Scheme 2

in Scheme 2, which is based on the structural information on **1**, **5**, and **6**; the upper part showing the structural consequences on the two salophen skeletons upon reduction, the lower part showing the corresponding chemical equations.

The starting material **1** is drawn as two overlapping non-bonded monomeric units, since we omitted for clarity the bridging oxygen interaction (see the structure of **4**). The introduction of two electrons into the dimer causes the reductive coupling of two imino groups across the two monomers with the consequent formation of a C–C bond (complex **5**).^{4,5} The structural analysis on **5** (*vide infra*) shows, however, that the C–C bond formation is accompanied by a change in the bonding mode of the salophen skeleton. Such a change in the bonding mode can be visualized by rotating the two oxygen arms

involved in the C–C bond formation in the opposite direction, as it can be easily followed using the oxygen labeling used in Scheme 2. At the same time the two related nitrogens display a bridging bond across the two Mn. The further introduction of two electrons leading from **5** to **6** has the same effect on the other pair of imino groups. The oxygen labeling in Scheme 2 shows that the four electron reduction causes not only the C–C bond formation but the formal exchange of the two salophen skeletons between the two Mn.

The anionic species depicted in Scheme 2 has been isolated as tight ion-pairs with sodium cations and with the stoichiometry shown at the bottom of the scheme. The synthesis of **6** has been carried out with a large excess of sodium metal, while the formation of **5** with controlled amounts of sodium is not

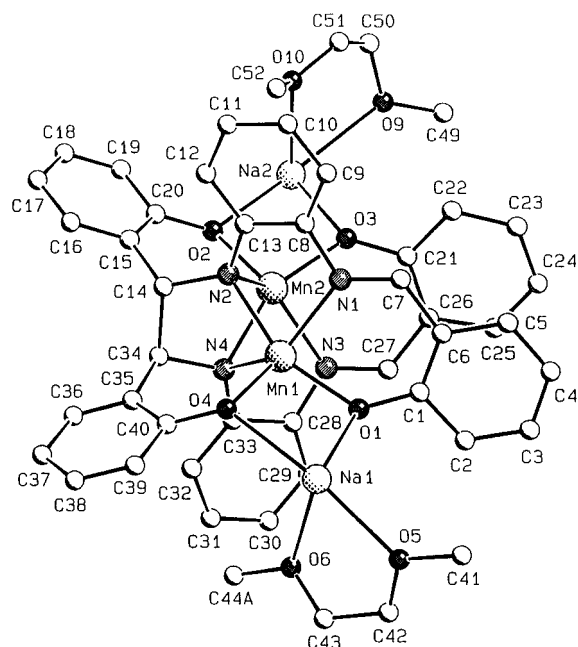


Figure 2. SCHAKAL view of complex **5**. The O7, O8, C45–C48 DME molecule bonded to Na2 and the B position of C44 are omitted for clarity.

particularly wise, because it should be separated from a mixture containing **6**. Independent high yield synthesis of **5** has been discovered (*vide infra*). Pure **5** undergoes reduction to **6**. The occurrence of a mixture of **5** and **6** even using limited amounts of Na suggests that the reduction of **5** to **6** is significantly faster than **1** to **5**. Both **5** and **6** have been fully characterized (see Experimental Section), including magnetic studies (see magnetic section) and an X-ray analysis. The structure of **5**, shown in Figure 2, displays the main features given in Scheme 2.

The C–C bond [C14–C34, 1.602(15) Å] bridging the two salophen units is particularly long, as is the case for very crowded structures. As a consequence of the sp^3 character of these imino carbons the phenolic rings O2, C15...C20 and O4, C35...C40 are nearly perpendicular to the remaining part of the salophen, the dihedral angles with N1, N2, O1, C1...C13 and N3, N4, O3, C35...C40 best planes being 105.5(2)° and 102.9(2)°, respectively. In such a conformation the planarity of the N₂O₂ salophen core is lost, and the ligand behaves as a tridentate N–N–O ligand toward one Mn and either O2 or O4 binds the adjacent manganese. Therefore the original salophen has been converted into the dinucleating hexa-anionic salophen₂ ligand. The two Mn achieve a trigonal bipyramidal coordination geometry thanks to the bridging bonding mode of N2 and N4.

The folding of salophen allowed the pair of atoms O2, O3 and O1, O4 to position at bite distances of 2.915(10) and 3.000(8) Å, respectively, thus functioning as bidentate ligands for Na2 and Na3 cations. Their coordination spheres are completed with DME molecules (see Figure S6). The structural Mn–N and Mn–O parameters do not show any particularity except for the rather short Mn1–N2 and Mn2–N4 [Mn–N_{av}, 2.138(5) Å] involving the anionic nitrogens (Table 2). The major structural changes on moving from **5** to **6** (Figure 3) have been depicted in Scheme 2.

The 2-fold coupled salophen moieties joined by two C–C bonds [C7–C14', 1.631(6) Å] form the centrosymmetric dinucleating octaanionic *salophen₂* ligand, which has been drawn without the metal centers in Figure 4.

The two centrosymmetric manganese atoms are bonded to the opposite sides of the centrosymmetric N4 planar core at distances ranging from 2.154(3) to 2.281(3) Å. The coordina-

Table 3. Selected Bond Distances (Å) and Angles (deg) for Complex **6**^a

Mn1–O1	2.171(4)	Na1–O5	2.481(6)
Mn1–O2	2.121(3)	Na1–O6	2.416(5)
Mn1–N1	2.258(3)	Na2–O1	2.459(4)
Mn1–N1'	2.174(4)	Na2–O2	2.460(4)
Mn1–N2	2.281(3)	Na2–O7	2.469(4)
Mn1–N2'	2.154(3)	Na2–O8	2.400(4)
Na1–O1	2.329(3)	O1–C1	1.330(5)
Na1–O2	2.391(3)	O2–C20	1.330(5)
Na1–O3	2.514(4)	C7–C14'	1.631(6)
Na1–O4	2.347(4)		
N2–Mn1–N2'	106.1(1)	O7–Na2–O8	68.1(1)
N1'–Mn1–N2'	70.6(1)	O2–Na2–O8	107.3(1)
N1'–Mn1–N2	68.5(1)	O2–Na2–O7	154.4(2)
N1–Mn1–N2'	69.3(1)	O1–Na2–O8	149.6(1)
N1–Mn1–N2	66.9(1)	O1–Na2–O7	105.1(1)
N1–Mn1–N1'	106.0(1)	O1–Na2–O2	65.4(1)
O2–Mn1–N2'	165.3(1)	Na1–O1–Na2	94.3(1)
O2–Mn1–N2	85.1(1)	Mn1–O1–Na2	87.3(1)
O2–Mn1–N1'	106.1(1)	Mn1–O1–Na1	89.7(1)
O2–Mn1–N1	124.7(1)	Na2–O1–C1	107.8(2)
O1–Mn1–N2'	102.6(1)	Na1–O1–C1	136.3(3)
O1–Mn1–N2	128.1(1)	Mn1–O1–C1	127.5(3)
O1–Mn1–N1'	163.3(1)	Na1–O2–Na2	92.7(1)
O1–Mn1–N1	84.7(1)	Mn1–O2–Na2	88.4(1)
O1–Mn1–O2	76.6(1)	Mn1–O2–Na1	89.3(1)
O5–Na1–O6	66.8(2)	Na2–O2–C20	111.4(3)
O4–Na1–O6	154.6(2)	Na1–O2–C20	135.2(3)
O4–Na1–O5	88.1(2)	Mn1–O2–C20	127.0(3)
O3–Na1–O6	112.1(2)	Mn1–N1–C8	102.0(2)
O3–Na1–O5	85.7(2)	Mn1–N1–C7	105.5(2)
O3–Na1–O4	67.5(1)	C7–N1–C8	128.3(3)
O2–Na1–O6	104.0(1)	Mn1–N1'–C7'	116.2(3)
O2–Na1–O5	117.0(2)	Mn1–N2–C14	104.6(2)
O2–Na1–O4	83.5(1)	Mn1–N2–C13	101.8(2)
O2–Na1–O3	142.9(1)	C13–N2–C14	127.5(3)
O1–Na1–O6	107.0(2)	Mn1–N2'–C14'	116.9(2)
O1–Na1–O5	172.2(2)	N1–C7–C6	118.5(3)
O1–Na1–O4	98.3(1)	C6–C7–C14'	109.2(3)
O1–Na1–O3	92.5(1)	N1–C7–C14'	107.0(3)
O1–Na1–O2	68.5(1)		

^a Prime denotes a transformation of $1 - x, y, 1 - z$.

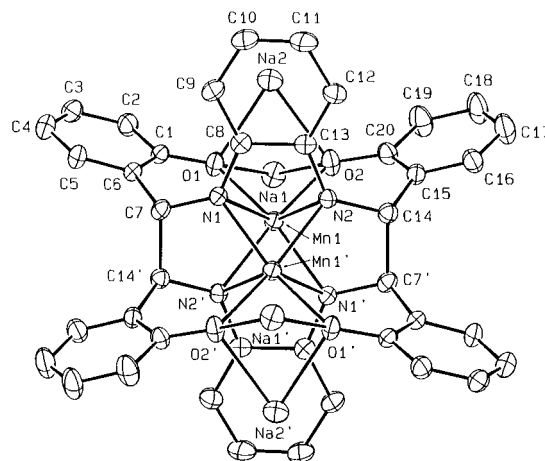


Figure 3. ORTEP view of complex **6** (30% probability ellipsoids). DME molecules bonded to sodium are omitted for clarity. Prime denotes a transformation of $1 - x, -y, 1 - z$.

tion around each metal is completed by two *cis* arranged oxygens [O1, O2 around Mn1] (Figure 5).

Referring to Figure 5, it should be mentioned (i) that Mn does not occupy the center of the prism, the displacements from the three faces O1, O2, N1, N2; O1, O2, N1', N2'; and N1, N2, N1', N2' being 0.988(1), 0.287(1), and 1.330(1) Å respectively; (ii) the Mn...Mn separation is 2.668(1) Å. Such a short metal-

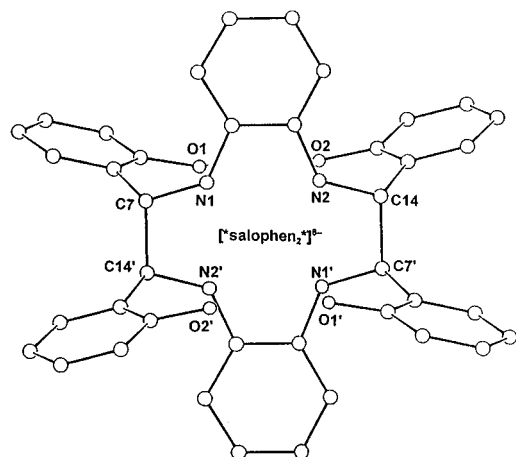


Figure 4. SCHAKAL view of the doubly C–C bond bridged salophen, *salophen**, in complex **6**.

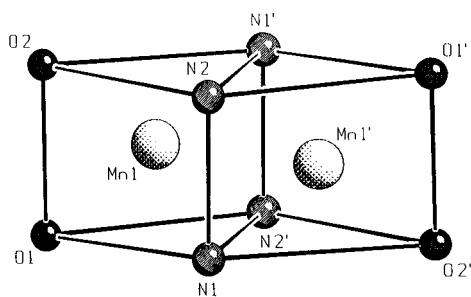


Figure 5. SCHAKAL drawing of coordination polyhedra around manganese cations in complex **6**.

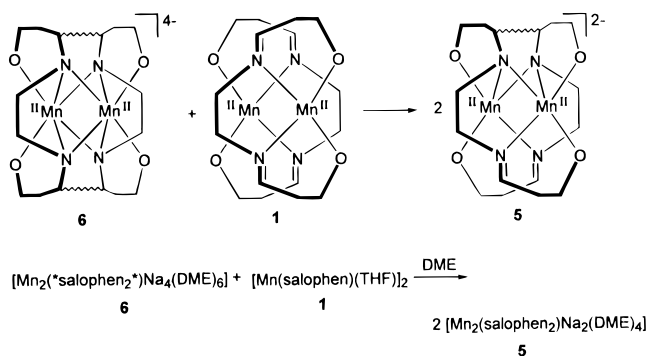
metal distance is particularly relevant in Mn dimers involved in redox processes.^{1d,12} The *salophen*₂* ligand defines an approximately planar 12-membered ring (see Figure 4) [maximum deviation 0.123(3) Å for N2] which is almost coplanar with the two *o*-phenyldiamine rings.

The N₂O₂ cores are almost perpendicular to the planar macrocyclic system [dihedral angle 89.4(1)°]. The conformation of the ligand allowed the O1 and O2 to function twice as a bidentate ligand for Na1 and Na2, which complete their coordination spheres with two and one DME molecules (not shown in Figure 3, see Figure S7), respectively. In the later case, the O₄ set is almost planar with Na2 displaced by 0.599(2) Å from it toward the C8···C13 ring, which is almost coplanar with the O₄ core [dihedral angle 8.5(1)°]. The rather short range of the Na2···C distances (from 2.834(5) to 3.288(6) Å) suggests a Na2···η⁶-(C8–C13) interaction, with a Na2···ring centroid separation of 2.715(5).¹³

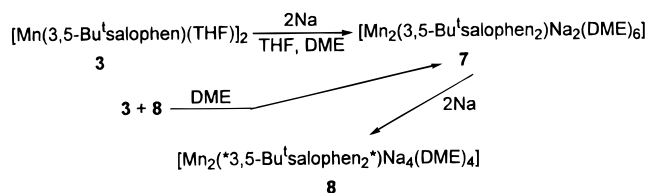
The search for an improved synthesis of **5** led us to discover a major property of the C–C bound Schiff base ligands. Mixing equimolar amounts of **1** and **6** in DME at room temperature leads to 90% of **5** as red violet crystals (Scheme 3), through the same steps discussed in detail in Scheme 2.

The occurrence of such a reaction is significant in many respects: (i) the C–C bond formation and cleavage is reversible (see the reduction of **5** to **6** and reaction in Scheme 3); (ii) the C–C bond functions as a shuttle of two electrons; and (iii) such an electron transfer can occur intermolecularly. As far as the latter point is concerned, we believe that the reaction between **1** and **6** is most probably assisted by the alkali cations which allow the two species to come in contact *via* coordination to the same sodium ions.

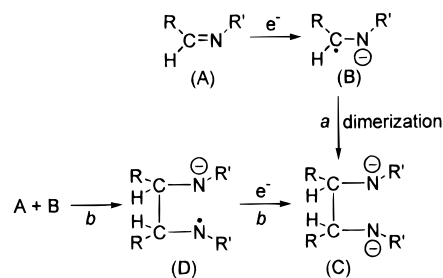
Scheme 3



Scheme 4



Scheme 5



We should mention at this point that the parallel synthetic pathway and redox behavior have been observed for the Bu^t substituted salophen–manganese complex **3**, as reported in Scheme 4.

The Bu^t substituents allowed us in many cases to better manage the solubility of such compounds, which are rather insoluble in the case of unsubstituted salophen.

Let us now discuss the genesis of our C–C coupled compounds. The best Schiff base which can be used for electronic reasons and its conformational characteristics is salophen (strictly planar), since the maximum of electronic delocalization is assured over the three conjugated aromatic rings. A rather obvious hypothesis is that, as in a normal pinacol reduction,¹⁴ which has in the present case the unusual characteristic of being reversible by the oxidative cleavage of the C–C bond, the reduction of the imino group leads to a radical anion either dimerizing to **C** (pathway *a*) or adding to an unreacted imino group to form a free radical to the nitrogen (pathway *b*, intermediate **D**) which is further reduced to **C**.

The key steps in both pathways *a* and *b* is the dimerization to produce **C** and **D**. Both dimerizations should suffer from steric hindrance at the imino carbons. For this reason we carried out the same reduction on **2**, where the imino hydrogens have been replaced by two methyl groups in the starting salophen ligand. The reduction of **2** carried out in THF with a rather

(12) (a) Manchanda, R.; Brudvig, G. W.; Crabtree, R. H. *Coord. Chem. Rev.* **1995**, *144*, 1. (b) Pecoraro, V. L.; Baldwin, M. S.; Gelasco, A. *Chem. Rev.* **1994**, *94*, 807.

(13) Weiss, E. *Angew. Chem., Int. Ed. Engl.* **1993**, *32*, 1501.

(14) (a) Allinger, N. *Org. Synth.* **1963**, *IV*, 840. (b) Bloomfield, J. J.; Owsley, D. C.; Ainsworth, C.; Robertson, R. E. *J. Org. Chem.* **1975**, *40*, 393. (c) Schreiber, A. A. P. *Tetrahedron Lett.* **1970**, 4271. (d) Smith, J. G.; Ho, I. *J. Org. Chem.* **1972**, *37*, 653. (e) Jaunin, R.; Höll, R. *Helv. Chim. Acta* **1958**, *41*, 1783. (f) Jaunin, R.; Magnenat, J.-P. *Helv. Chim. Acta* **1959**, *42*, 328. (g) Bastian, J.-M.; Jaunin, R. *Helv. Chim. Acta* **1963**, *46*, 1248. (h) Shono, T.; Kise, N.; Okazaki, E. *Tetrahedron Lett.* **1992**, *33*, 3347.

Scheme 6

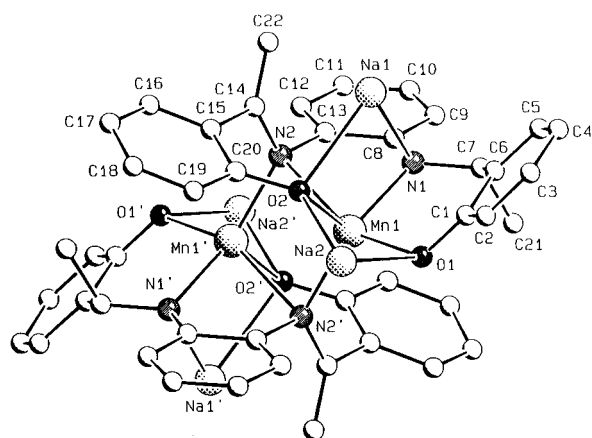
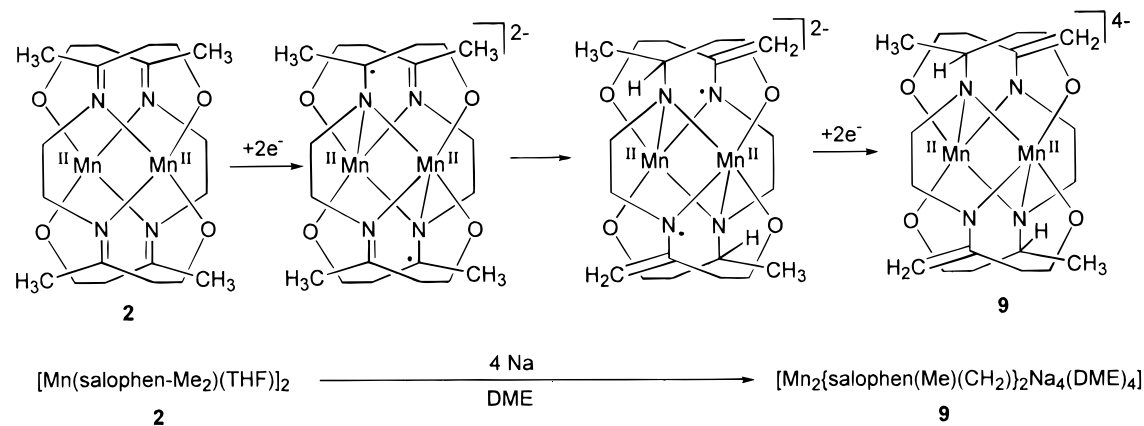


Figure 6. SCHAKAL view of complex **9**. DME molecules bonded to sodium are omitted for clarity. Prime denotes a transformation of $-x$, $-y$, $1 - z$.

large excess of sodium metal gave **9** as a yellow crystalline solid upon recrystallization from DME. In this case, the preliminary generation of a radical anion is not followed by any dimerization, rather the radical at the carbon abstracts a hydrogen atom from a methyl group either of the same or of the other salophen of the dimer, to give a methylene and leading to the rearrangement shown in Scheme 6.

The bonding scheme displayed in Scheme 6 for **9** is based on the X-ray structure reported in Figure 6.

The centrosymmetric dimer contains two $[\text{Mn}(\text{salophen})]$ units, with the presence of a methyl substituent at C7 [C7–C21, 1.515(7) Å] and a methylene group at C14 [C14–C22, 1.354(8) Å]. The latter one forms with the adjacent C14–N2 [1.392(6) Å] a sort of azaallyl fragment, while C7–N1 is reduced to a single bond [1.445(7) Å]. Dimerization occurs through the amido N2 which bridges asymmetrically the two Mn atoms, which are at a distance of 3.050(1) Å [Mn1–N2, 2.440(4) Å; Mn1–N2', 2.104(4) Å]. The coordination geometry around the metal is a distorted trigonal bipyramid with N1, O2, and N2 in the axial positions. Na1 (bonded to O1 and O2) and Na2 (bonded to O2 and N1) are in a pseudotetrahedral environment (see Figure S9) completed by a DME molecule. The structural parameters not mentioned above do not deserve any particular comment (Table 4).

The temperature dependence of the magnetic moment of compounds **5–8** indicates antiferromagnetically coupled Mn(II) dimers. The best fitting values for **5** and **6** are $g = 2.02$, $J = -43.0 \text{ cm}^{-1}$, $x = 3.9\%$ and $g = 1.97$, $J = -40.8 \text{ cm}^{-1}$, $x = 0.4\%$, respectively. The exchange constant values found for

Table 4. Selected Bond Distances (Å) and Angles (deg) for Complex **9**^a

Mn1–O1	2.116(4)	Na2–O6	2.355(5)
Mn1–O2	2.119(3)	O1–C1	1.317(7)
Mn1–N1	2.088(5)	O2–C20	1.338(6)
Mn1–N2	2.440(4)	N1–C7	1.445(7)
Mn1–N2'	2.104(4)	N1–C8	1.381(7)
Na1–O2	2.598(4)	N2–C13	1.451(8)
Na1–O3	2.387(5)	N2–C14	1.392(6)
Na1–O4	2.265(4)	C6–C7	1.530(8)
Na1–N1	2.444(4)	C7–C21	1.515(7)
Na2–O1	2.386(5)	C14–C15	1.480(9)
Na2–O2	2.265(4)	C14–C22	1.354(8)
Na2–O5	2.484(6)		
N2–Mn1–N2'	96.0(1)	Na2–O1–C1	108.3(3)
N1–Mn1–N2'	138.2(2)	Mn1–O1–C1	121.7(3)
N1–Mn1–N2	74.3(1)	Na1–O2–Na2	117.8(1)
O2–Mn1–N2'	108.7(1)	Mn1–O2–Na2	95.1(1)
O2–Mn1–N2	82.7(1)	Mn1–O2–Na1	79.6(1)
O2–Mn1–N1	110.2(1)	Na2–O2–C20	123.7(3)
O1–Mn1–N2'	108.7(1)	Na1–O2–C20	108.1(2)
O1–Mn1–N2	154.7(1)	Mn1–O2–C20	124.8(3)
O1–Mn1–N1	90.1(1)	Mn1–N1–Na1	83.9(2)
O1–Mn1–O2	84.2(1)	Na1–N1–C8	109.4(3)
O4–Na1–N1	153.6(2)	Na1–N1–C7	105.1(3)
O3–Na1–N1	102.3(2)	Mn1–N1–C8	114.7(3)
O3–Na1–O4	72.2(2)	Mn1–N1–C7	119.4(3)
O2–Na1–N1	86.3(1)	C7–N1–C8	117.5(4)
O2–Na1–O4	99.1(2)	Mn1–N2–C14	111.8(3)
O2–Na1–O3	171.1(2)	Mn1–N2–C13	102.2(3)
O5–Na2–O6	68.2(2)	C13–N2–C14	114.0(4)
O2–Na2–O6	179.7(2)	N1–C7–C6	111.6(4)
O2–Na2–O5	112.0(2)	C6–C7–C21	111.0(4)
O1–Na2–O6	104.5(2)	N1–C7–C21	114.7(4)
O1–Na2–O5	154.0(2)	N2–C14–C22	125.3(5)
O1–Na2–O2	75.2(1)	N2–C14–C15	115.2(5)
Mn1–O1–Na2	91.8(1)	C15–C14–C22	119.4(5)

^a Prime denotes a transformation of $-x$, $-y$, $1 - z$.

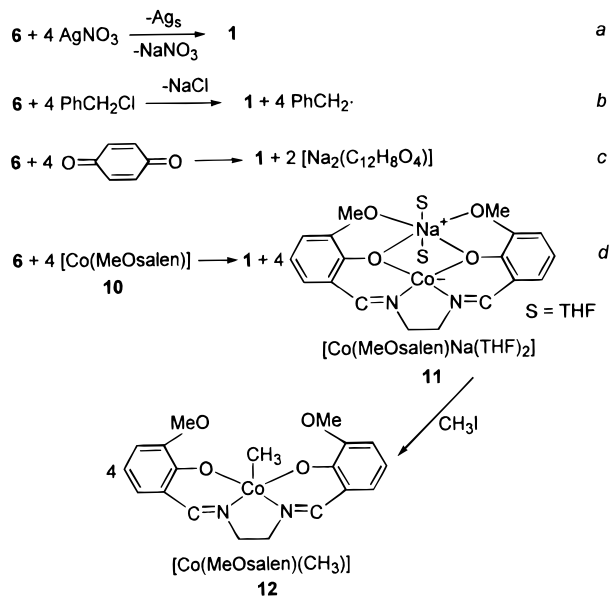
5–8 show fairly strong antiferromagnetic coupling for these μ -amido Mn(II) dimers.¹¹ It is worth noting that these values are higher than those observed for μ -hydroxo, μ -alkoxo, μ -phenoxo, and μ -carboxylato Mn(II)–Mn(II) dimers (with exchange coupling constants of few cm^{-1}) intensively studied^{1c,15–17} within the investigation of inorganic model complexes of manganese-containing metalloproteins.^{1c}

(15) Wiegardt, K.; Bossek, U.; Nuber, B.; Weiss, J.; Bonvoisin, J.; Corbella, M.; Vitols S. E.; Girerd, J.-J. *J. Am. Chem. Soc.* **1988**, *110*, 7398.

(16) Menage, S.; Vitols, S. E.; Bergerat, P.; Codjovi, E.; Kahn, O.; Girerd, J.-J.; Guillot, M.; Solans X.; Calvet, T. *Inorg. Chem.* **1991**, *30*, 2666.

(17) Wiegardt, K.; Bossek, K.; Bonvoisin, J.; Beauvillain, P.; Girerd, J.-J.; Nuber, B.; Weiss J.; Heinze, J. *Angew. Chem., Int. Ed. Engl.*, **1986**, *25*, 1030.

Scheme 7



3. The C–C Bonds Functioning as Two Electron Reservoirs. The most attractive property of complexes **5–8** is their tendency to function as reducing agents. In the first class we report reactions in which only the electrons stored in the C–C bonds are used in combination with inorganic, organic, and organometallic substrates,¹⁸ as exemplified in Scheme 7.

The slow addition of AgNO_3 or PhCH_2Cl to **6** reveals the intermediacy of a violet solution, complex **5**, before giving a solution containing exclusively **1**. Such reagents reverse the reduction pathway given in Scheme 2. In the case of benzyl chloride, the excess of reagent does not cause any oxidation of Mn(II), contrary to what has been reported for iron(II)–Schiff base derivatives.¹⁹ In reaction *b*) the benzyl radical has been partially identified as 1,2-diphenylethane. The reaction of **6** with *p*-benzoquinone can be easily followed by the appearance of the insoluble blue-green sodium salt of quinidrone.²⁰ The reaction of **6** with the cobalt(II)–Schiff base **10** is very fast in THF and led to a deep green solution of the corresponding cobalt(I) derivative,^{4d,21} **11**. The latter compound was easily identified *via* its conversion into the corresponding organometallic derivative, **12** (see the Experimental Section).²² The preliminary interaction with the reducible substrate is easily understandable in the case of reactions *a* and *b*, while we should admit, in the case of reaction *d* and *c*, the electron transfer pass through the interaction assured by the ability of **10** and

(18) Connelly, N. G.; Geiger, W. E. *Chem. Rev.* **1996**, *96*, 877.

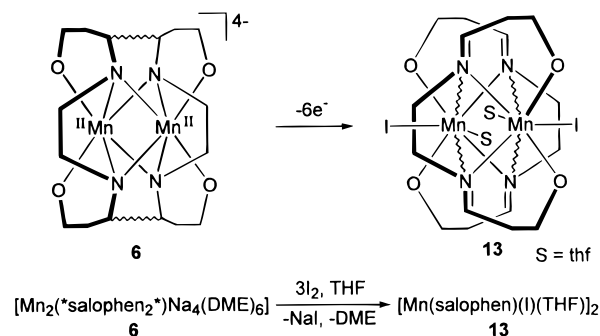
(19) Floriani, C.; Fachinetti, G. *J. Chem. Soc., Chem. Commun.* **1973**, 17.

(20) Depew, M. C.; Wan, J. K. S. in *The Chemistry of Quinonoid Compounds*; Patai, I., Rappaport, Z., Eds; Wiley: New York, 1988; Vol. 21.

(21) Fachinetti, G.; Floriani, C.; Zanazzi, P. F.; Zanzari, A. R. *Inorg. Chem.* **1979**, *18*, 3469.

(22) (a) Swamy, R. L. In *Comprehensive Organometallic Chemistry II*; Abel, E. W., Stone, F. G. A., Wilkinson, G., Eds.; Pergamon: Oxford, U.K., 1995; Vol. 8; Chapter 1, p 42, and references therein. (b) Calligaris, M.; Randaccio, L. In *Comprehensive Coordination Chemistry*; Wilkinson, G., Gillard, R. D., McCleverty, J. A., Eds.; Pergamon: Oxford, U.K., 1987. (c) Pratt, J. M.; Craig, P. J. *Adv. Organomet. Chem.* **1973**, *11*, 404. (d) Calligaris, M.; Nardin, G.; Randaccio, L. *Coord. Chem. Rev.* **1972**, *7*, 385. (e) Bigotto, A.; Costa, G.; Mestroni, G.; Pellizzer, G.; Puxeddu, A.; Reisenhofer, E.; Stefani, L.; Tauzher, G. *Inorg. Chim. Acta* **1970**, *4*, 41. (f) Pattenden, G. *Chem. Soc. Rev.* **1988**, *17*, 361 and references therein. (g) Dodd, D.; Johnson, M. D. *J. Organomet. Chem.* **1973**, *52*, 1. (h) Pratt, J. M.; Craig, P. J. *Adv. Organomet. Chem.* **1973**, *11*, 414. (i) Randaccio, L.; Bresciani-Pahor, N.; Zangrando, E.; Marzilli, L. G. *Chem. Soc. Rev.* **1989**, *18*, 225. (j) Charlaud, J.-P.; Zangrando, E.; Bresciani-Pahor, N.; Randaccio, L.; Marzilli, L. G. *Inorg. Chem.* **1993**, *32*, 4256.

Scheme 8



p-benzoquinone to bind alkali cations. The four reactions in Scheme 7 have some common characteristics.

(i) They use exclusively the C–C bonds as a source of electrons with [Mn(salophen)] being restored in its original form, thus reversing the steps in Scheme 2. The simple cleavage of the C–C and Mn–N bonds as they are in **6** would lead to an overall migration of a salophen ligand from one Mn to the other one.

(ii) The reaction with a reducible substrate never occurs at the C–C sites, thus supporting a long range electron transfer process, mediated by the metal sites in the structure.

A second class of reactions considers substrates which are able not only to use the electrons from the C–C bonds but also from Mn increasing its oxidation state.

The reaction of **6** with a stoichiometric amount of iodine led to the corresponding Mn(III) derivative **13** (see Scheme 8), which was converted, in the presence of a large excess of iodine, to the triiodide derivative **14**, [Mn(salophen)(I₃)(THF)], whose structural parameters and figure are given in the Supporting Information. The same products **13** and **14** have been obtained by a direct oxidation of **1** with iodine.

The reaction of manganese(II) with dioxygen assisted by an intramolecular source of electrons, other than the metal, represents a novel approach in the vast area of manganese complexes reacting with O₂.^{1d,12b,15,23} This approach opens new perspectives in modeling studies concerning the Mn-assisted oxygen transfer reactions.²⁴ In addition, to couple a metal with a source of electrons would engender a novel hypothesis on how to manage the redox chemistry of a transition metal in general.^{12a,15,25}

In this context we studied the reaction of dioxygen with **6** and **8**, though the use of **8** was more favorable due to its considerable solubility in hydrocarbons. The results on the two compounds were quite the same. In the reaction with O₂ [O₂: Mn = 1:1], complexes **6** and **8** behave as eight electron reducing agents, four of which come from the two C–C bonds and four from the oxidation of Mn(II) to Mn(IV), with the concomitant reduction of dioxygen to oxide. Complex **16** was freed from Na₂O by extracting the crude product with *n*-hexane, though

(23) (a) Coleman, W. M.; Taylor, L. T. *Coord. Chem. Rev.* **1980**, *32*, 1. (b) Horwitz, C. P.; Dailey, G. C.; *Comments Inorg. Chem.* **1993**, *14*, 283. (c) Bossek, U.; Weyhermüller, T.; Wieghardt, K.; Nuber, B.; Weiss, J. J. *Am. Chem. Soc.* **1990**, *112*, 6387.

(24) (a) Yamada, T.; Imagawa, K.; Nagata, T.; Mukaiyama, T. *Chem. Lett.* **1992**, 2231. (b) Mukaiyama, T.; Yamada, T.; Nagata, T.; Imagawa, K. *Chem. Lett.* **1993**, 327. (c) Nagata, T.; Imagawa, K.; Yamada, T.; Mukaiyama, T. *Inorg. Chim. Acta* **1994**, *220*, 283. (d) Nagata, T.; Imagawa, K.; Yamada, T.; Mukaiyama, T. *Chem. Lett.* **1994**, 1259. (e) Imagawa, K.; Nagata, T.; Yamada, T.; Mukaiyama, T. *Chem. Lett.* **1995**, 335. (f) MacDonnel, F. M.; Fackler, N. L. P.; Stern, C.; O'Halloran, T. V. *J. Am. Chem. Soc.* **1994**, *116*, 7431. (g) Nagata, T.; Imagawa, K.; Yamada, T.; Mukaiyama, T. *Bull. Chem. Soc. Jpn.* **1995**, *68*, 3241.

(25) (a) Brudvig, G. W.; Crabtree, R. H. *Proc. Natl. Acad. Sci. U.S.A.* **1986**, *83*, 4586. (b) Brudvig, G. W.; Crabtree, R. H. *Progress in Inorganic Chemistry*; 1989; Vol. 37. (c) Dismukes, G. C. *Chem. Scr.* **1988**, *28A*, 99.

Table 5. Comparison of Relevant Structural Parameters within the Mn(salophen) Units for Complexes 4–6, 9

		4 ^a		5 ^b		6	9
dist of atoms from the N ₂ O ₂ core, Å	O1	0.038(13)	[0.050(13)]	0.072(6)	[0.132(7)]	0.021(3)	0.233(3)
	O2	−0.038(13)	[−0.054(13)]	−0.334(7)	[−0.166(5)]	−0.021(3)	−0.218(3)
	N1	−0.085(17)	[−0.107(16)]	−0.771(1)	[−0.890(8)]	−0.022(3)	−0.469(4)
	N2	0.125(20)	[0.116(17)]	0.808(7)	[0.756(7)]	0.022(3)	0.452(4)
	Mn1	−0.019(3)	[−0.021(3)]	0.846(2)	[0.864(2)]	−0.988(1)	0.830(1)
folding ^c along the N1...O1 line, deg		26.6(6)	[25.2(6)]	18.5(3)	[20.6(3)]	35.1(1)	9.0(2)
folding along the N2...O2 line, deg		7.2(7)	[1.0(5)]	32.8(3)	[50.4(3)]	38.0(1)	15.7(2)
angle between Mn1–N1–O1 and Mn1–N2–O2 planes, deg		6.2(6)	[6.8(5)]	84.1(2)	[76.1(3)]	74.8(1)	73.3(1)
angle between the mean OC ₃ N planes, deg		19.8(6)	[24.2(6)]	74.4(3)	[75.4(3)]	2.8(1)	62.2(2)
torsion angle N1–C8–C13–N2, deg		4(3)	[−5(3)]	−6.0(13)	[−9.9(12)]	0.4(5)	−3.4(7)
dist of atoms from the Mn1–N1–N2 plane, Å	C8	0.12(2)	[0.14(2)]	0.484(11)	[0.449(10)]	1.067(4)	0.677(5)
	C13	0.69(2)	[0.09(2)]	0.530(10)	[0.575(9)]	1.068(3)	0.656(5)

^a Values in square brackets refer to molecule B. ^b Values in square brackets refer to Mn2, O3, O4, N3, N4, C28, C33. ^c The folding is defined as the dihedral angle between the Mn, N, O, and OC₃N planes of a six-membered chelation ring.

Table 6. Experimental Data for the X-ray Diffraction Studies on Crystalline Complexes 4–6, 9, and 14^a

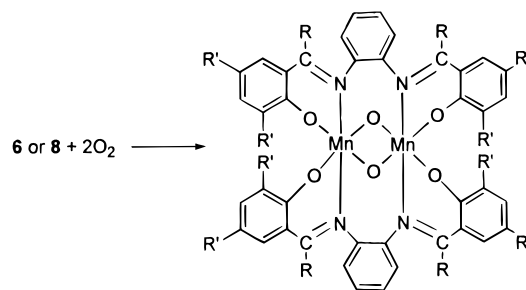
complex	4	5	6	9	14
chemical formula	C ₅₀ H ₃₈ Mn ₂ N ₆ O ₄	C ₅₂ H ₅₈ Mn ₂ N ₄ Na ₂ O ₁₀	C ₆₄ H ₈₈ Mn ₂ N ₄ Na ₄ O ₁₆	C ₆₀ H ₇₆ Mn ₂ N ₄ Na ₄ O ₁₂	C ₂₄ H ₂₂ I ₃ MnN ₂ O ₃ C ₄ H ₈ O
<i>a</i> (Å)	24.632(4)	14.241(3)	12.678(3)	13.303(3)	9.886(8)
<i>b</i> (Å)	16.821(3)	16.080(4)	18.314(3)	17.456(4)	19.377(3)
<i>c</i> (Å)	10.098(3)	12.426(2)	14.807(2)	14.039(3)	15.883(4)
α (deg)	90	101.91(2)	90	90	90
β (deg)	90	111.42(2)	92.83(2)	104.56(2)	94.47(3)
γ (deg)	90	88.71(2)	90	90	90
<i>V</i> (Å ³)	4184.0(16)	2587.6(10)	3433.8(11)	3155.4(12)	3033(3)
<i>Z</i>	4	2	2	2	4
fw	896.8	1054.9	1371.3	1247.1	894.2
space group	<i>P</i> 2 ₁ 2 ₁ 2 ₁	<i>P</i> 1	<i>P</i> 2 ₁ / <i>n</i>	<i>P</i> 2 ₁ / <i>n</i>	<i>P</i> 2 ₁ / <i>n</i>
<i>T</i> (°C)	22	22	22	22	22
λ (Å)	0.71069	1.54178	0.71069	0.71069	0.71069
ρ _{calcd} (g cm ^{−3})	1.424	1.354	1.326	1.313	1.958
μ (cm ^{−1})	6.31	46.41	4.40	4.68	34.74
transmission coeff	0.885–1.000	0.820–1.000	0.828–1.000	0.934–1.000	0.691–1.000
unique measured data	7274	9751	6092	5531	5372
unique “observed” data	3336	7403	5006	4423	4299
criterion for obsn	<i>F</i> ² > 2σ(<i>F</i> ²)	<i>F</i> ² > 0	<i>F</i> ² > 0	<i>F</i> ² > 0	<i>F</i> ² > 0
unique obs data [<i>I</i> > σ2(<i>I</i>)]	1819	2728	2818	2016	2416
<i>R</i> =	0.046	0.074	0.045	0.044	0.045
<i>wR</i> 2 =	0.137	0.222	0.131	0.108	0.129
GOF =	1.353	0.979	0.989	0.804	1.027

^a *R* = Σ|Δ*F*|/Σ|*F*_o| calculated on the unique observed data [*I* > 2σ(*I*)]. *wR*2 = [Σ*w*|Δ*F*²|/Σ*w*|*F*_o²|]^{1/2} calculated on the unique “observed” data. GOF = [Σ*w*|Δ*F*²|/(*NO* − *NV*)]^{1/2}.

this was impossible for **15** due to its low solubility in hydrocarbons.

Complex **15** has been very recently reported as the unexpected result from the reaction of salophenH₂ and KMnO₄.²⁶ An analogous structure appeared on a substituted salen made from some Mn(III) oxidation.²⁷ Complex **16** has been fully characterized, including the X-ray analysis, and shows a similar structure to **15**, and it has been included in the Supporting Information. The reaction shown in Scheme 9 is peculiar in that the obtention of a di-μ-oxo-manganese(IV) occurs directly from Mn(II) and dioxygen, and because the binucleating bonding mode of salophen requires a partial migration of the ligand across two Mn ions. The kind of synthesis reported for the two μ-dioxo-Mn(IV) having the skeleton shown for **15** and **16**^{26,27} is serendipitous and so not particularly informative on their genesis.

As far as the first issue is concerned, we know that the reaction of either **1** or **4** with dioxygen results in the oxidation

Scheme 9

R' = R = H; [Mn₂(μ-salophen)₂(μ-O)₂], **15**

R = H; R' = Bu^t; [Mn₂(μ-3,5-Bu^t-salophen)₂(μ-O)₂], **16**

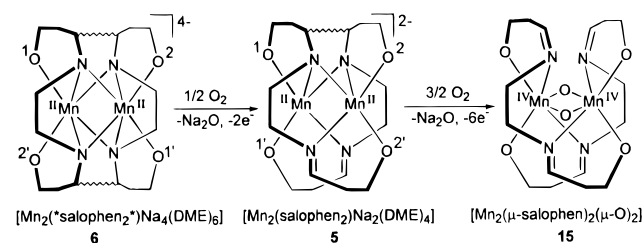
of the imino to an amido carbon, with the concomitant formation of a polymeric μ-hydroxo-Mn(III).²⁸ This proves that the reaction of **6** and **8** with dioxygen does not reverse the reduction pathway shown in Scheme 2 and that the reaction of O₂ does not occur on **1**. Therefore, unlike for the reactions reported in Scheme 7, the reaction of **6** and **8** with O₂ does not restore the

(26) Torayama, H.; Nishide, T.; Asada, H.; Fujiwara, M.; Matsushita, T. *Chem. Lett.* **1996**, 387–388.

(27) Bermejo, M. R.; Castiñeiras, A.; Garcia-Monteagudo, J. C.; Rey, M.; Sousa, A.; Watkinson, M.; McAuliffe, C. A.; Pritchard, R. G.; Beddoes, R. L. *J. Chem. Soc., Dalton Trans.* **1996**, 2935–2944.

(28) Gallo, E.; Solari, E.; Re, N.; Floriani, C.; Chiesi-Villa, A.; Rizzoli, C. *Angew. Chem., Int. Ed. Engl.* **1996**, 35, 1981–1983.

Scheme 10



original $[\text{Mn}(\text{salophen})]$ fragment for further reactivity with O_2 . In addition, the reaction with O_2 does not result in the cleavage of the intradimer C–C and Mn–N bonds in **6–8**, since the final compounds would have a salophen to Mn bonding mode different from that observed in **15** and **16**. This bonding mode is compatible with the assumption that **5** and **7** are the precursors of **15** and **16** in the reaction with O_2 . Reacting **6** with a controlled amount of dioxygen gave **5** as violet crystals (see the Experimental Section). This proves that the intermediate compound reacting with O_2 and leading directly to **15** is complex **5** and not **1**. Further, the salophen ligand has in **5** and **7** the bridging bonding mode displayed in **15** and **16**. The reaction pathway of **6**, which will be the same for **8**, is shown in Scheme 10. The sequence shows the two electron oxidation of **6** to **5**, followed by the cleavage of two Mn–N and one C–C bonds in **5** with the incorporation of two bridging oxo ligands. Therefore the relative arrangement of the salophen ligand toward Mn in **15** remains as it is in **5**, with salophen displaying a bridging bonding mode across two Mn ions.

The temperature dependence of the magnetic moment of **15** and its *tert*-butyl derivative **16** are quite similar and indicate antiferromagnetically coupled Mn(IV) dimers. The data were fitted using a Heisenberg Hamiltonian, with $S_1 = S_2 = 3/2$, and including a correction for monomeric Mn(IV) impurities.¹¹ The best fitting values for **16** are $g = 1.86$, $J = -80.1 \text{ cm}^{-1}$, and $x = 1.8\%$. The antiferromagnetic coupling constant obtained for these bis μ -oxo Mn(IV) dimers are similar to those observed for other bis μ -oxo Mn(IV) Schiff base dimers (usually *ca.* 100 cm^{-1}) with comparable Mn–Mn distance.^{1c,29}

Conclusions

This report deals with a rather unique investigation on the chemical reduction of the very popular model Mn(II)-tetradentate Schiff base complexes. This approach led us to discover (i) a novel mode of storing and releasing electrons based on the metal-assisted reversible formation (reductive coupling) and cleavage (oxidative decoupling) of C–C bonds across two Schiff base ligands; (ii) the coupling of an electron reservoir centered at the ligand with the redox behavior of the metal. This kind of molecular battery has some original peculiarities: (a) the C–C bonds function as a shuttle of two electrons without being involved in a reaction; (b) a large number of electrons can be stored and released by the system; (c) the metal assists long-range electron transfers from the C–C bonds to the incoming substrates; and (d) the two redox systems, the metal and the ligand, can function independently from another or synergically.

Experimental Section

General Procedure. Unless otherwise noted, materials were obtained from commercial suppliers and used without further purification. Solvents were dried and distilled by standard methods prior to use. The syntheses of $[\text{Mn}_3\text{Mes}_6]\cdot\text{toluene}$ ⁷ and 3,5-Bu₂-salicylaldehyde

have been carried out as reported.³⁰ All compounds were handled using modified Schlenk techniques under a nitrogen atmosphere or in an inert atmosphere drybox under nitrogen. IR spectra were recorded on a Perkin-Elmer 1600 FT IR instrument.

Magnetic susceptibility measurements were made on a with a MPMS5 SQUID susceptometer (Quantum Design Inc.) operating at a magnetic field strength of 3 kG. Corrections were applied for diamagnetism calculated from Pascal constants. Effective magnetic moments were calculated by the equation $\mu_{\text{eff}} = 2.828(\chi_{\text{Mn}}T)^{1/2}$, where χ_{Mn} is the magnetic susceptibility per manganese atom. Fitting of the magnetic data to the theoretical equation were performed by minimizing the agreement factor, defined as

$$R = \sum_i \frac{[\chi_i^{\text{obsd}}T - \chi_i^{\text{calcd}}T]^2}{(\chi_i^{\text{obsd}}T)^2}$$

through Levenberg–Marquardt routine.³¹

Synthesis of 1. $[\text{Mn}_3\text{Mes}_6]\cdot\text{C}_7\text{H}_8$ ⁷ (7.1 g, 7.31 mmol) was added to a THF (500 mL) solution of salophenH₂ (6.90 g, 21.8 mmol) to give an orange solution which then turned deep red. The mixture was then refluxed for 12 h and concentrated to $1/3$ of its volume, and pentane (150 mL) was added. The resulting red crystalline solid was collected by filtration and dried *in vacuo* (7.10 g, 73%), Crystals suitable for X-ray analysis were obtained recrystallizing **1** from CH₃CN, to give the solvated form, $[\text{Mn}(\text{salophen})(\text{CH}_3\text{CN})_2]$. Anal. Calcd for **1**, C₄₈H₄₄Mn₂N₄Na₄O₆: C, 65.31; H, 5.02; N, 6.35. Found: C, 65.13; H, 5.14; N, 6.72. IR (Nujol, $\nu_{\text{max}}/\text{cm}^{-1}$) 1609(s), 1581(s), 1528(m), 1296(m), 1178(s), 1145(s), 972(w), 914(m), 884(w), 852(w), 747(s), 529(m). UV–vis (THF, $8.10 \times 10^{-5} \text{ M}$): $\lambda = 252 \text{ nm}$ ($\epsilon = 71\,700 \text{ cm}^{-1} \text{ M}^{-1}$), 298 (43\,700), 410 (46\,500).

Synthesis of 2. $[\text{Mn}_3\text{Mes}_6]\cdot\text{C}_7\text{H}_8$ ⁷ (4.67 g, 4.81 mmol) was added to a THF (300 mL) solution of salophen(CH₃)₂H₂ (4.96 g, 14.4 mmol) to give an orange solution which then turned deep red. The mixture was then refluxed for 12 h and concentrated to $1/3$ of its volume, and pentane (150 mL) was added. The resulting orange crystalline solid was collected by filtration and dried *in vacuo* (5.00 g, 74%). Anal. Calcd for **2**, C₅₂H₅₂Mn₂N₄O₆: C, 66.52; H, 5.58; N, 5.97. Found: C, 67.31; H, 5.30; N, 6.45. IR (Nujol, $\nu_{\text{max}}/\text{cm}^{-1}$) 1599(s), 1583(s), 1546(s), 1530(s), 1469(s), 1440(s), 1310(s), 1213(s), 1130(m), 861(m), 752(s), 738(m). $\mu = 5.92 \mu_{\text{B}}$ at 298 K.

Synthesis of 3. NaH (1.56 g, 65.0 mmol) was added slowly (*ca.* 3 min) without stirring, to an orange THF (400 mL) solution of salophen-(Bu)₄H₂ (16.0 g, 29.6 mmol). Gas evolution was immediately observed, with the concomitant formation of an orange suspension. The mixture was stirred at room temperature until gas evolution stopped (*ca.* 10 min) and then refluxed for 3 h. The excess NaH was removed by filtration, and $[\text{MnCl}_2(\text{THF})_{1.5}]_n$ (6.92 g, 29.6 mmol) was added. The resulting red suspension was refluxed overnight and then evaporated to dryness, and the residue was extracted with toluene (250 mL) to eliminate NaCl. The suspension was evaporated to dryness, *n*-hexane (150 mL) added, and the red crystalline solid was collected by filtration and dried *in vacuo* (17.33 g, 88%). Anal. Calcd for **3**, C₈₀H₁₀₈Mn₂N₄O₆: C, 72.16; H, 8.17; N, 4.21. Found: C, 72.22; H, 8.66; N, 4.31. IR (Nujol, $\nu_{\text{max}}/\text{cm}^{-1}$) 1600(s), 1577(s), 1544(m), 1524(s), 1433(s), 1381(s), 1359(s), 1254(m), 1166(s), 832(m), 784(m), 746(s), 508(m).

Synthesis of 4. Complex **1** (1.65 g, 1.87 mmol) was dissolved in pyridine (50 mL), the red solution was stirred at room temperature for 12 h and then evaporated to dryness, and pentane (50 mL) was added. The resulting red solid was collected by filtration and dried *in vacuo* (1.50 g, 90%). Recrystallization from Et₂O:Py = 80:20 gave crystals suitable for X-ray analysis. Anal. Calcd for **4**, C₅₀H₃₆Mn₂N₆O₄: C, 66.97; H, 4.27; N, 9.37. Found: C, 66.83; H, 4.11; N, 9.20. IR (Nujol, $\nu_{\text{max}}/\text{cm}^{-1}$) 1606(s), 1580(s), 1540(s), 1525(s), 1482(m), 1387(s), 1349(m), 1327(m), 1301(s), 1252(w), 1243(w), 1216(w), 1176(s), 1145(s), 1124(m), 1037(m), 1028(m), 918(m), 841(m), 798(m), 771(m), 752(s), 740(s), 701(s), 600(m), 529(s), 460(m).

(30) Lorrow, J. F.; Jacobsen, E. N.; Gao, Y.; Hong, Y.; Nie, X.; Zepp, C. M. *J. Org. Chem.* **1994**, *59*, 1939.

(31) Press, W. H.; Flannery, B. P.; Teukolsky, S. A.; Vetterling, W. T. *Numerical Recipes*; Cambridge University Press: Cambridge, U.K., 1989.

(29) Libby, E.; Webb, R. J.; Streib, W. E.; Folting, K.; Huffman, J. C.; Hendrickson, D. N.; Christou, J. *Inorg. Chem.* **1989**, *28*, 4037.

Synthesis of 5. Method A. Sodium sand (0.30 g, 13.0 mmol) was added to a suspension of **1** (0.82 g, 0.93 mmol) in DME (300 mL). The resulting red suspension was stirred at room temperature for 12 h, the excess sodium then removed by extraction, the filtrate was concentrated to $1/3$ of its volume and a dilute mixture of P_2O_5 -dried oxygen in nitrogen atmosphere allowed to enter. After 3 days red crystals suitable for X-ray analysis was obtained and collected by filtration (0.6 g, 56%). Anal. Calcd for **5**, $C_{56}H_{68}Mn_2N_4Na_2O_{12}$: C, 58.74; H, 5.99; N, 4.89. Found: C, 57.81; H, 5.32; N, 5.37. IR (Nujol, ν_{max}/cm^{-1}) 1600(s), 1580(s), 1533(m), 1441(s), 1338(s), 1315(m), 1292(s), 1264(s), 1167(s), 1148(m), 1109(m), 1086(s), 1031(m), 902(m), 752(s), 548(w), 477(w).

Method B. Complex **6** (0.99 g, 0.72 mmol) was added as a solid to a DME (150 mL) suspension of **1** (0.64 g, 0.72 mmol), the resulting red solution was stirred at room temperature for 12 h and then concentrated to $1/3$ of its volume, and *n*-hexane (100 mL) was added. The resulting red crystalline solid was collected by filtration and dried *in vacuo* (1.5 g, 90%). Recrystallization from DME gave crystals suitable for X-ray analysis. Anal. Calcd for **5**, $C_{56}H_{68}Mn_2N_4Na_2O_{12}$: C, 58.74; H, 5.99; N, 4.89. Found: C, 58.62; H, 5.17; N, 5.22. UV-vis (THF, 6.73×10^{-5} M): $\lambda = 248$ nm (ϵ 70 600 $cm^{-1} M^{-1}$), 290 (41 700), 394 (25 900).

Synthesis of 6. Sodium sand (1.72 g, 74.78 mmol) was added to a suspension of **1** (9.02 g, 10.23 mmol) in THF (350 mL). The resulting red suspension was stirred at room temperature for 12 h, then the excess sodium was removed by filtration, and the filtrate evaporated to dryness. DME (30 mL) and *n*-hexane (200 mL) was added. The resulting yellow solid was collected by filtration and dried *in vacuo* (12.2 g, 87%). Recrystallization from DME gave crystals suitable for X-ray analysis. Anal. Calcd for **6**, $C_{64}H_{88}Mn_2N_4Na_4O_{16}$: C, 56.06; H, 6.47; N, 4.09. Found: C, 56.49; H, 6.06; N, 4.56. IR (Nujol, ν_{max}/cm^{-1}) 1587(s), 1544(m), 1440(s), 1286(s), 1261(s), 1109(m), 1083(m), 1034(m), 1022(m), 754(m). UV-vis (THF, 5.47×10^{-5} M): $\lambda = 244$ nm (ϵ 62 500 $cm^{-1} M^{-1}$), 298 (39 600), 378(sh) (12 000), 508 (3400).

Synthesis of 7. Complex **8** (1.67 g, 1.02 mmol) was added as a solid to a DME (100 mL) suspension of **3** (1.36 g, 1.02 mmol), the resulting red solution was stirred at room temperature for 12 h and then concentrated to $1/3$ of its volume, and the resulting red crystalline solid was collected by filtration and dried *in vacuo* (2.5 g, 70%). Anal. Calcd for **7**, $C_{96}H_{152}Mn_2N_4Na_2O_{16}$: C, 64.99; H, 8.64; N, 3.16. Found: C, 64.37; H, 8.70; N, 3.01.

Synthesis of 8. Sodium sand (0.69 g, 30.0 mmol) was added to a suspension of **3** (7.47 g, 5.62 mmol) in DME (100 mL). The resulting red suspension was stirred at room temperature for 12 h, and the excess sodium was removed by extraction. The mixture was then concentrated to $1/3$ of its volume, and heptane (100 mL) was added. The resulting yellow solid was collected by filtration and dried *in vacuo* (6.0 g, 65%). Recrystallization from DME gave crystals suitable for X-ray analysis. Anal. Calcd for **8**, $C_{88}H_{132}Mn_2N_4Na_4O_{12}$: C, 64.45; H, 8.11; N, 3.42. Found: C, 64.87; H, 8.42; N, 3.07. IR (Nujol, ν_{max}/cm^{-1}) 1593(m), 1542(s), 1407(m), 1358(s), 1347(s), 1309(s), 1276(s), 1244(s), 1193(s), 1156(m), 1123(m), 1082(s), 1020(m), 862(s), 834(s), 736(m), 724(s).

Synthesis of 9. Sodium sand (0.46 g, 20.0 mmol) was added to a suspension of **2** (1.96 g, 2.09 mmol) in THF (200 mL). The resulting red suspension was stirred at room temperature for 12 h, the excess sodium was removed by filtration, and the mixture was evaporated to dryness. DME (30 mL) and heptane (100 mL) were then added. The resulting yellow solid was collected by filtration and dried *in vacuo* (2.0 g, 77%). Recrystallization from DME gave crystals suitable for X-ray analysis. Anal. Calcd for **9**, $C_{60}H_{76}Mn_2N_4Na_4O_{12}$: C, 57.79; H, 6.14; N, 4.49. Found: C, 57.84; H, 6.45; N, 4.43. IR (Nujol, ν_{max}/cm^{-1}) 1581(s), 1537(m), 1431(s), 1290(s), 1241(s), 1191(m), 1107(m), 1081(s), 1033(m), 858(m), 748(s). $\mu = 3.15 \mu_B$ at 293 K.

Reaction of Complex 6 with $AgNO_3$. Complex **6** (1.04 g, 0.76 mmol) was added as a solid to a THF (150 mL) suspension of $AgNO_3$ (0.52 g, 3.04 mmol). The resulting red suspension was stirred at room temperature for 12 h and refluxed for 3 h. The metallic silver and $NaNO_3$ were removed by filtration, and the red solution concentrated to $1/3$ of its volume followed by the addition of *n*-hexane (100 mL). The resulting orange solid was collected by filtration and dried *in vacuo* (0.40 g, 60%). Anal. Calcd for **1**, $C_{48}H_{44}Mn_2N_4O_6$: C, 65.31; H, 5.02; N, 6.35. Found: C, 64.78; H, 4.53; N, 6.63.

Reaction of Complex 6 with $PhCH_2Cl$. To a red benzene (50 mL) suspension of **6** (0.98 g, 0.71 mmol) was added, in a dropwise manner and at room temperature, a benzene (50 mL) solution of a fresh distilled $PhCH_2Cl$ (0.57 mL, 4.94 mmol). The resulting red suspension was stirred at room temperature for 12 h and refluxed for 4 h. The $NaCl$ was eliminated by filtration, the solution evaporated to dryness, and pentane (100 mL) was added. The resulting red solid was collected by filtration and dried *in vacuo* (0.50 g, 78%). Anal. Calcd for [Mn(salophen)(benzene)], $C_{26}H_{20}MnN_2O_2$: C, 69.80; H, 4.51; N, 6.26. Found: C, 69.34; H, 4.96; N, 5.49. IR (Nujol, ν_{max}/cm^{-1}) 1608(s), 1533(s), 1314(m), 1272(w), 1179(m), 1150(m), 1030(w), 917(w), 853(w), 751(s), 699(m), 601(w), 542(w).

Reaction of Complex 6 with 1,4-Benzoquinone. To a THF (150 mL) solution of **6** (3.33 g, 2.43 mmol) was added solid 1,4-benzoquinone (1.36 g, 12.58 mmol). The resulting green suspension was stirred at room temperature for 1 h and then refluxed for 12 h. The green complex [(1,4-benzoquinone)-(1,4- Na_2 -hydroquinone)] was eliminated by extraction and identified by elemental analysis. The resulting red solution was evaporated to dryness, pentane (100 mL) added, and the resulting orange solid collected by filtration and dried *in vacuo* (0.60 g, 78%). Anal. Calcd for **1**, $C_{48}H_{44}Mn_2N_4O_6$: C, 65.31; H, 5.02; N, 6.35. Found: C, 65.50; H, 4.33; N, 6.25.

Synthesis of 12. The complex [Co{salen(OCH₃)₂}] (0.66 g, 1.72 mmol) was added as a solid to a THF (150 mL) suspension of **6** (1.18 g, 0.86 mmol). The resulting green solution was stirred at room temperature for 12 h, and a THF (50 mL) solution of CH_3I (0.364 g, 2.58 mmol) was added in a dropwise manner at -60 °C. The resulting red solution was stirred at room temperature for 12 h and evaporated to dryness, then the red residue dissolved in CH_2Cl_2 (100 mL) and then was poured into distilled water. The organic phase was collected, and the water was eliminated by azeotropic distillation. After 1 day at -20 °C, a red crystalline solid was collected by filtration and dried *in vacuo* (0.5 g, 62%). 1H NMR for [Co{salen(OCH₃)₂}](CH_2Cl_2), $C_{20}H_{23}Cl_2CoN_2O_4$, (DMSO-*d*₆, 298 K): δ 7.90 (s, 2H); 6.76–6.65 (m, 4H); 6.30–6.27 (m, 2H); 5.76 (s, 2H); 3.74 (s, 6H); 3.44–3.35 (m, 4H); 2.15 (s, 3H).

Synthesis of 13. To a stirred red THF (50 mL) solution of **6** (0.95 g, 0.70 mmol) was added, at -60 °C, a THF solution of I_2 (58 mL, 0.04 M). The resulting red suspension was stirred at room temperature for 12 h to give a red crystalline solid which was then collected by filtration and dried *in vacuo* (0.67 g, 84%). Anal. Calcd for **13**, $C_{24}H_{22}IMn_2N_2O_3$: C, 50.72; H, 3.90; N, 4.93. Found: C, 50.05; H, 4.13; N, 4.73. IR (Nujol, ν_{max}/cm^{-1}) 1603(s), 1577(s), 1535(s), 1437(s), 1286(m), 1234(m), 1194(s), 1150(s), 1129(m), 872(m), 812(s), 761(s), 543(s). $\mu = 4.72 \mu_B$ at 293 K.

Synthesis of 14. To a stirred red THF (50 mL) solution of **6** (0.82 g, 0.60 mmol) was added, at -60 °C, a THF (50 mL) solution of I_2 (1.37 g, 5.40 mmol). The resulting red suspension was stirred at room temperature for 12 h and evaporated to dryness, and Et_2O (100 mL) was added. The red crystalline solid was collected by filtration and dried *in vacuo* (0.8 g, 88.8%). Anal. Calcd for **14**, $C_{24}H_{22}I_3Mn_2N_2O_3$: C, 35.06; H, 2.70; N, 3.41. Found: C, 35.73; H, 3.07; N, 3.35. IR (Nujol, ν_{max}/cm^{-1}) 1604(s), 1574(s), 1534(s), 1311(m), 1284(m), 1195(m), 1151(m), 1129(m), 1102(m), 812(m), 753(m), 544(m). $\mu = 5.02 \mu_B$ at 293 K.

Synthesis of $15 \cdot 2Na_2O$. Complex **6** (6.65 g, 4.85 mmol) was dissolved in pyridine (150 mL) to which was added anhydrous oxygen. The resulting brown solution was stirred at room temperature for 12 h and concentrated to $1/3$ of its volume, and *n*-hexane (100 mL) was added. The resulting brown solid was collected by filtration and dried *in vacuo* (4.1 g, 87%). Anal. Calcd for $15 \cdot 2Na_2O$, $C_{44}H_{36}Mn_2N_4Na_4O_9$: C, 54.67; H, 3.75; N, 5.80. Found: C, 54.03; H, 3.90; N, 5.48.

Synthesis of 16. Complex **8** (1.1 g, 0.67 mmol) was dissolved in pyridine (100 mL) to which was added anhydrous oxygen. The resulting brown solution was stirred at room temperature for 12 h and then evaporated to dryness. Pentane (50 mL) was added to the residue, and the brown crystalline solid formed was collected by filtration and dried *in vacuo* (0.6 g, 56%). Recrystallization from *n*-hexane gave crystals suitable for X-ray analysis. Anal. Calcd for **16**, $C_{88}H_{132}Mn_2N_4O_{14}$: C, 66.90; H, 8.42; N, 3.55. Found: C, 66.29; H, 7.18; N, 3.61.

X-ray Crystallography for Complexes 4–6, 9, and 14. Suitable crystals were mounted in glass capillaries and sealed under nitrogen.

The reduced cells were obtained with use of TRACER.³² Crystal data and details associated with data collection are given in Tables 6 and S1 (Supporting Information). Data for all complexes were collected at room temperature (295 K) on a single-crystal diffractometer (Philips PW1100 for **4**, Rigaku AFC6S for **5**, **6** and **14** and Enraf-Nonius CAD4 for **9**). For intensities and background, individual reflection profiles were analyzed.³³ The structure amplitudes were obtained after the usual Lorentz and polarization corrections,³⁴ and the absolute scale was established by the Wilson method.³⁵ The crystal quality was tested by ψ scans showing that crystal absorption effects could not be neglected. Data were then corrected for absorption with ABSORB³⁶ for **9** and using a semiempirical method³⁷ for **4–6**, and **14**. Anomalous scattering corrections were included in all structure factor calculations.^{38b} Scattering factors for neutral atoms were taken from ref 38a for nonhydrogen atoms and from ref 39 for H.

Structure solutions were based on the observed reflections [$I > 2\sigma(I)$]. The refinements were carried out using the unique reflections with $F^2 > 0$ for **5**, **6**, **9**, and **14** and with $F^2 > -2\sigma(F^2)$ for **4**. The structures were solved by the heavy-atom method starting from a three-dimensional Patterson map.⁴⁰ During the least-squares the function minimized was $\sum w(\Delta F^2)^2$.⁴¹ In the last stage of refinement the weighting scheme $w = 1/[\sigma^2(F_o^2) + (aP)^2]$ (with $P = (F_o^2 + 2F_c^2)/3$) was applied with a resulting in the value of 0.0274, 0.0959, 0.0620, 0.0369, for **4–6**, **9**, and **14**, respectively.

(32) Lawton, S. L.; Jacobson, R. A. "TRACER", a cell reduction program; Ames Laboratory: Iowa State University of Science and Technology, 1965.

(33) Lehmann, M. S.; Larsen, F. K. *Acta Crystallogr. Sect. A: Cryst. Phys. Diffr. Theor. Gen. Crystallogr.* **1974**, *A30*, 580.

(34) Data reduction, structure solution, and refinement were carried out on a Quansan personal computer equipped with an INTEL Pentium processor and on an Encore 91 computer.

(35) Wilson, A. J. C. *Nature (London)* **1942**, *150*, 151.

(36) Ugozzoli, F. *Comput. Chem.* **1987**, *11*, 109.

(37) North, A. C. T.; Phillips, D. C.; Mathews, F. S. *Acta Crystallogr., Sect. A: Cryst. Phys., Diffr., Theor. Gen. Crystallogr.* **1968**, *A24*, 351–359.

(38) *International Tables for X-ray Crystallography*; Kynoch Press: Birmingham, England, 1974; Vol. IV, (a) p 99, (b) p 149.

(39) Stewart, R. F.; Davidson, E. R.; Simpson, W. T. *J. Chem. Phys.* **1965**, *42*, 3175.

(40) Sheldrick, G. M. *SHELX76, Program for crystal structure determination*, University of Cambridge: Cambridge, England, 1976.

Refinement of all complexes was carried out first isotropically and then anisotropically for all the non-H atoms, except for the C44 methyl carbon atom in **5**, which was found to be statistically distributed over two positions (A and B) isotropically refined with site occupation factors of 0.6 and 0.4, respectively. The refinement of the THF molecule of crystallization in **14** was carried out by constraining the C–O and C–C distances to be 1.42(1) and 1.54(1) Å, respectively.

The hydrogen atoms, except those associated to the disordered C44 methyl carbon in **5**, which were ignored, partly located from difference maps, partly put in geometrically calculated positions, were introduced prior to the final refinements as fixed atom contributions with isotropic U 's fixed at 0.08 Å² for **4**, 0.10 Å² for **5**, **6**, and **9**, and 0.12 Å² for **14**.

The final difference maps showed no peaks having chemical meaning above the general background.

Final atomic coordinates are listed in Tables S2–S5 for non-H atoms and in Tables S8–S11 for hydrogens. Thermal parameters are given in Tables S14–S17, and bond distances and angles are given in Tables S20–S23.⁴²

Acknowledgment. We would like to thank the "Fonds National Suisse de la Recherche Scientifique" (Bern, Switzerland, Grant No. 20-40268.94) and Ciba-Geigy (Basel, Switzerland) for financial support.

Supporting Information Available: Description of the structure for complex **14**. X-ray crystallography for complex **16**. Supplementary drawings for **4–6**, **9**, **14**, and **16**. Tables giving crystal data and details of the structure determination, fractional atomic coordinates, bond lengths, bond angles, anisotropic thermal parameters, and hydrogen atom locations for **4–6**, **9**, **14**, and **16**. Magnetic properties of dimeric manganese complexes; plots of magnetic susceptibilities and μ_B for **3**, **5**, **6**, **16** (50 pages). See any current masthead page for ordering and Internet access instructions.

JA9640962

(41) Sheldrick, G. M. *SHELXL92, Program for crystal structure refinement*; University of Göttingen, Göttingen, Germany, 1992.

(42) See the paragraph at the end of the paper regarding the Supporting Information.